

ChemComm

Accepted Manuscript



This is an *Accepted Manuscript*, which has been through the Royal Society of Chemistry peer review process and has been accepted for publication.

Accepted Manuscripts are published online shortly after acceptance, before technical editing, formatting and proof reading. Using this free service, authors can make their results available to the community, in citable form, before we publish the edited article. We will replace this *Accepted Manuscript* with the edited and formatted *Advance Article* as soon as it is available.

You can find more information about *Accepted Manuscripts* in the [Information for Authors](#).

Please note that technical editing may introduce minor changes to the text and/or graphics, which may alter content. The journal's standard [Terms & Conditions](#) and the [Ethical guidelines](#) still apply. In no event shall the Royal Society of Chemistry be held responsible for any errors or omissions in this *Accepted Manuscript* or any consequences arising from the use of any information it contains.

Ni-promoted Synthesis of Graphitic Carbon Nanotubes from *in situ* Produced Graphitic Carbon for Dehydrogenation of Ethylbenzene

Cite this: DOI: 10.1039/x0xx00000x

Jing Wang, Zhongzhe Wei, Yutong Gong, Shiping Wang, Diefeng Su, Chuanlong Han, Haoran Li, Yong Wang*

Received 00th January 2015,
Accepted 00th January 2015

DOI: 10.1039/x0xx00000x

www.rsc.org/

Graphitic carbon nanotubes (GCNT) were fabricated from *in situ* produced graphitic carbon by calcining biomass/melamine/Ni(NO₃)₂·6H₂O. Ni-based hybrids (NiO_x@GCNT) displayed superior catalytic capacity in direct dehydrogenation of ethylbenzene. The specific reaction rate can reach up to 8.1 μmolm⁻²h⁻¹, and unprecedented stability was obtained over 165 h without any activation process.

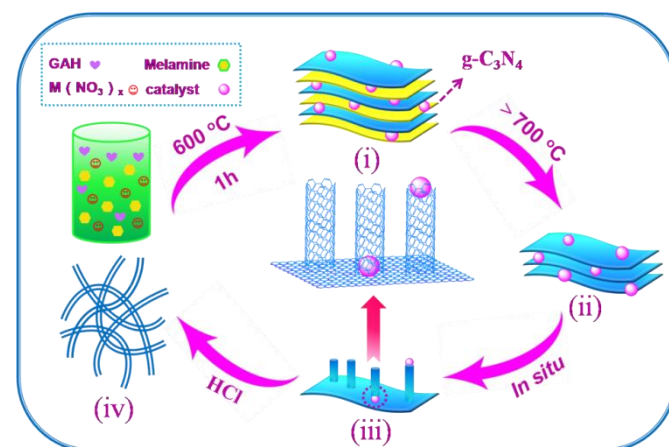
Carbon nanomaterials are ubiquitous in diverse technological and energy-related applications because of their wide availability and superior properties.¹ Particularly, carbon nanotubes (CNTs) are hailed as a rapidly rising star in materials science. Owing to their extraordinary geometric arrangement of carbon atoms and superior electronic properties,² CNTs not only offer an ideal playground for exploring the properties of 1D tubular materials, but can also be used in fuel cells,³ biological probes,⁴ and chemical catalysis.⁵

Normally, CNTs are produced by means of arc-discharge,⁶ laser ablation methods,⁷ and chemical vapor deposition (CVD).⁸ Although the arc-discharge and laser ablation techniques generate thin CNTs, these processes have very limited ability to control the growth of fibers and other unwanted deposits.⁹ Up till now, CVD method is the predominant technique. Comparing with arc-discharge and laser ablation, the CVD methods can produce relatively large amounts of CNTs with controlled size and growth density. And yet for all that, one key drawback is that it is only appropriate for gasification of small molecules. Biomass materials cannot replicate the traditional CVD process to CNTs production. In addition, low space-time-yield, low selectivity for graphitic carbon, and high operational costs are also main disadvantages. To circumvent these drawbacks, researchers embarked on a concerted effort to explore efficient approaches to synthesize CNTs.¹⁰ Templates strategy (e.g., carbon nanorings were employed as templates for the synthesis of CNTs) has attracted significant interest.¹¹ It is worth mentioning that carbon source for the growth of nanotubes by microwave irradiation

technology or CVD methods were also introduced.¹² Notwithstanding these advances, warranting the cost-effective manufacture of CNTs still remains a crucial challenge.

It has been well established that whatever the technique was employed, iron-family elements are efficient catalysts for the preparation of CNTs.¹³ Generally, these catalysts are prepared by co-precipitation of the metal precursors. The manufacturing process is complicated and the morphology and particle size of the catalyst have to be well controlled. Herein, we develop an efficient strategy for the growth of carbon nanotubes. Ni(NO₃)₂·6H₂O, Fe(NO₃)₃·9H₂O, and Co(NO₃)₂·6H₂O were used as catalysts as delivered without any further treatment. D-glucosamine hydrochloride (GAH), a most widely available biomass, was utilized as both the C and N sources. Melamine, a common and cheap industrial chemical, played the part of artificial template for the temporary preparation of graphitic carbon. After a carbonization of the GAH/melamine/nitrate mixture, amounts of graphitic carbon nanotubes (GCNT) were readily formed. Different from the CNTs made by traditional CVD method, the sidewalls of GCNT are comprised of crumpled graphene-like nanosheets. The inner diameter ranges from ~50-70 nm, which is larger than commercial CNTs (~7 nm). Additionally, doping with electron-rich N atoms in GCNT makes it possible to control electronic properties and consequently enhanced catalytic performance.

The fabrication of GCNT was diagrammed in Scheme 1. Based on the experimental analysis, we conjectured that the evolution of



Scheme 1. Scheme for the fabrication of GCNT.

Advanced Materials and Catalysis Group, Center for Chemistry of High-performance and Novel Materials, Department of Chemistry, Zhejiang University, Hangzhou, 310028 (P. R. China)

E-mail: chemwy@zju.edu.cn

†Electronic Supplementary Information (ESI) available. See DOI: 10.1039/b000000x/

GCNT was achieved by the following process: (i) Thermal condensation of melamine formed layered graphitic carbon nitride ($g\text{-C}_3\text{N}_4$)¹⁴ and GAH was condensed to carbon skeleton in the interlayer of the $g\text{-C}_3\text{N}_4$.¹⁵ Synchronously, nitrate underwent dehydration, decomposition and *in situ* nucleation into the hybrids. (ii) High temperature annealing led to the thermal decomposition of $g\text{-C}_3\text{N}_4$, during which new atoms (C, N) produced, and the latest graphene-like sheets were liberated. The structural defects in the graphene sheets may lead to the formation of broken sites, where C, N atoms can dissolve into the catalyst nanoparticles and then precipitate to form new graphene layers.^{8e} (iii) The generated active nanoparticles fluctuated inside the solid phase and catalyzed the growth of NiO_x @GCNT from graphitic carbon. Meanwhile, the growth of new graphene layers lifted up the original graphene layers and resulted in wrinkles in the nanotubes. (iv) Further acid treatment, GCNT can be readily achieved.

The structure of GCNT was investigated by scanning electron microscopy (SEM). As illustrated in Figure 1a, b, the sample was totally composed of ultralong graphitic carbon nanotubes. The length of GCNT can reach microns. Transmission electron microscopy (TEM) further revealed that the inner diameter of GCNT is ~50-70 nm (Figure 1c, d), which is larger than commercial CNTs (~7 nm) (Figure S1, see the Supporting Information). Naturally, such intrinsic features will promote its application in catalysis. High-resolution transmission electron microscopy (HRTEM) images (Figure 1e, f) further disclosed the high crystallinity characters of GCNT. Interestingly, the sidewalls of as-synthesized GCNT exhibit an irregular and corrugated graphene-like morphology with a layer spacing of ~0.2-0.3 nm. Such unique structure maybe a result inheriting from the parent graphitic carbon.

Moreover, doping N atoms into graphitic carbon texture can affect

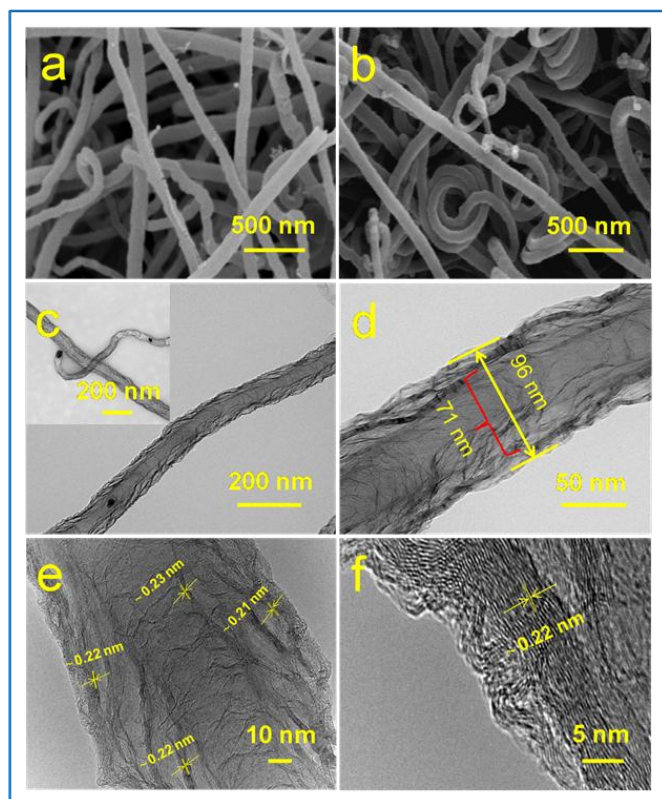


Figure 1. a, b) SEM images of GCNT at different regions. c, d) TEM images of GCNT at different magnifications. e, f) HRTEM images of GCNT at different magnifications. GCNT was prepared by thermal condensation of GAH, melamine, and $\text{Ni}(\text{NO}_3)_2 \cdot 6\text{H}_2\text{O}$ (mass ratio GAH:melamine:Ni=1:20:1.1) at 1000 °C for 1 h, and then treated by HCl.

physicochemical properties of CNTs, thus improving their performance.¹⁶ The chemical status of N was validated by X-ray photoelectron spectroscopy (XPS). As shown in Figure S2a, the high-resolution N 1s spectra of GCNT displayed three principle types of nitrogen coordination, corresponding to graphitic quaternary N, pyrrole N, and pyridine N. Pyridine N has been proposed an essential component in generating bamboo-like structures,¹⁷ which is consistent with TEM data. The textural properties of GCNT were then measured by N_2 adsorption-desorption analysis, and concluded in Table S1. The adsorption isotherm resembled type IV with a hysteresis loop, corresponding to the existence of mesopores (Figure S3a), which is beneficial for catalytic process. Raman spectra were also collected to further assess their graphitic structure. For comparison, the graphitic carbon nanomaterials (GCN) prepared by thermal condensation of GAH/melamine were demonstrated.¹⁵ As shown in Figure S2b, the I_D/I_G ratio of GCNT ($I_D/I_G=0.68$) significantly decreased in comparison to GCN ($I_D/I_G=1.02$), implying the higher graphitization degree of GCNT. It is noteworthy that a well-defined 2D peak, which gives information about the degree of nanotube crystallinity,¹⁸ was also observed in GCNT. However, it was not appeared in GCN, suggesting the high crystallinity of GCNT. X-ray diffraction (XRD) further investigates the crystallographic structure of GCNT (Figure S2c). The prominent peak at 26° was recorded and ascribed to the (002) reflection of the graphite-type lattice. Apart from the characteristic peaks of graphitic carbon, there were still weak peaks, which can be assigned to Ni/NiO (Ni: PDF 65-2865, NiO: PDF 65-5745). Remarkably, the intensity of graphite (002) vastly enhanced comparing with GCN, further validating that the graphitization degree of GCNT was significantly improved. Besides, electrical conductivity measurement also indicated the good conductivity of GCNT (Table S2).

To unveil the growth mechanism, correlations among the composition, pyrolysis temperature and holding time were then systematically elucidated. As for control experiments, micro-scale bulk substance with very little uneven tubes was detected when GAH mixed with $\text{Ni}(\text{NO}_3)_2 \cdot 6\text{H}_2\text{O}$ (Figure S4a, b). In the case of GAH/melamine, graphene-like GCN was formed (Figure S4c, d). Once pyrolysis of $\text{Ni}(\text{NO}_3)_2 \cdot 6\text{H}_2\text{O}$ with melamine, both a large range of connected carbon spheres and partial small diameter nanotubes were observed (Figure S4e, f). Whereas pyrolyzed the mixture of GAH/melamine/Ni, a wide range of graphitic carbon nanotubes were produced with larger diameter (Figure 1). From these results, one can conclude that GAH, melamine, and $\text{Ni}(\text{NO}_3)_2 \cdot 6\text{H}_2\text{O}$ are all indispensable for the formation of uniform, large diameter GCNT.

In an attempt to deeply clarify the role of each component, the mission of melamine was explored firstly. As exhibited in Figure S5, GCN displayed a regular morphology transition from sponge-like graphitic carbon to homogeneous, sheet-like nanostructure with the increase of melamine amount.¹⁹ When $\text{Ni}(\text{NO}_3)_2 \cdot 6\text{H}_2\text{O}$ was added into the above mentioned systems, much morphology changed. In the case of GAH:melamine:Ni=1:5:1.1, plenty of protrusions, i.e. baby nanotubes, formed on the surface of sponge graphitic carbon (Figure S5d). Once increase the proportion of melamine, large-scale baby nanotubes grew out of the thick sheets, and the length of nanotubes obviously increased (Figure S5e). Further enhance the amount of melamine, uniform, ultralong graphitic carbon nanotubes were synthesized on a larger scale (Figure S5f). Based on these observations, it is undoubtedly that the evolution of carbon morphology greatly depends on the amount of melamine, i.e., the early formation of flake-like graphitic carbon helps to realize the uniform growth of GCNT.

In addition to the effect of melamine, the growth of GCNT can be finely controlled by tuning the concentration of $\text{Ni}(\text{NO}_3)_2 \cdot 6\text{H}_2\text{O}$. As demonstrated in Figure S6a, low content of $\text{Ni}(\text{NO}_3)_2 \cdot 6\text{H}_2\text{O}$ seems

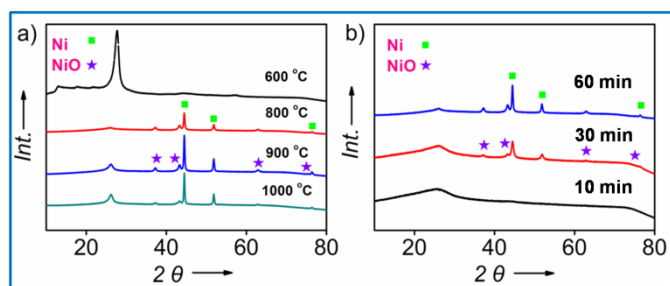


Figure 2. a) XRD patterns of products (mass ratio GAH:melamine:Ni=1:20:1.1) at different calcination temperature for 1 h. b) XRD patterns of products (mass ratio GAH:melamine:Ni=1:20:1.1, 800 °C) with different holding time. All the samples were not treated with HCl.

cannot realize the radical conversion from graphitic carbon to nanotubes, only minor baby nanotubes appeared. Increasing the $\text{Ni}(\text{NO}_3)_2 \cdot 6\text{H}_2\text{O}$ dosage from 0.95 g to 1.1 g to 1.6 g, typical GCNT was obtained (Figure S6b, S6c, S6d). Based on these observations, it has been found that the amount of $\text{Ni}(\text{NO}_3)_2 \cdot 6\text{H}_2\text{O}$ not only controlled the density of active sites, but also determined the impetus to promote nanotubes growing from graphitic carbon. Calcination technology also exhibited the similar morphology evolution process. As presented in Figure S7, a whole range of flake-like structure was formed at 600 °C, which was the composite of g- C_3N_4 and condensed GAH. The presence of g- C_3N_4 was verified by two signals present on the XRD pattern (Figure 2a), namely the strong shoulder peak at 2θ of 27.6°, and the low-angle diffraction peak at 2θ of 13.1°. Further raising the pyrolysis temperature to 800 °C, g- C_3N_4 underwent complete thermolysis, and the resulting material exhibited large range plates with protuberances. Once increasing the pyrolysis temperature from 900 to 1000 °C, the proportion of GCNT dramatically lifted (Figure S7). According to the XRD data (Figure 2a), the peak signals of Ni-based particles gradually enhanced with increasing temperature, indicating the fluctuation of Ni-based particles. It is thus reasonable to speculate that the enhanced calcination temperature benefits the migration of metal particles, thus greatly improved the growth rate of tubes.

To shed more light on the growth mechanism, the initial growth of GCNT was determined by intentional tuning the holding time. Figure 3 highlights the sequence of GCNT formation at 800 °C.

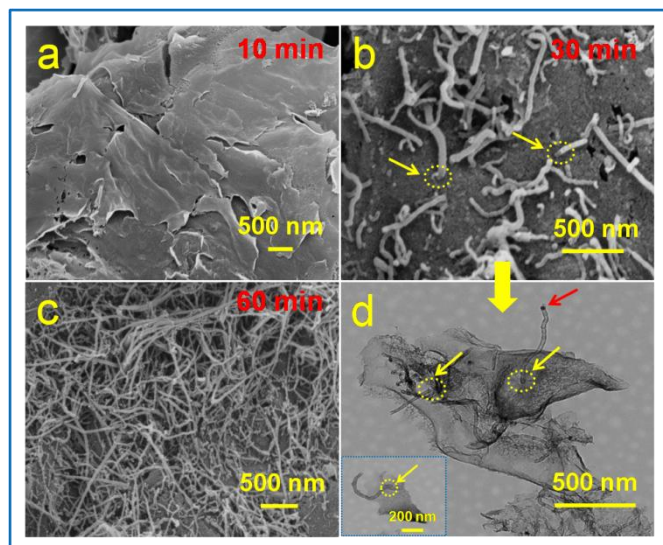


Figure 3. a), b), c) SEM recorders for products (mass ratio GAH:melamine:Ni=1:20:1.1, 800 °C, treatment with HCl) with different holding time. d) TEM image for product from b).

Within 10 minutes, a large amount of lamellar morphology was formed. Increasing the holding time to 30 minutes, large range plates were observed with protuberances, which were the baby GCNT. TEM images (Figure 3d) further disclosed that GCNT was directly developed from graphitic carbon. The yellow arrows and circles signify the root regions of GCNT, where they connect to the graphene plane. During the growth, Ni-based particles may be firstly encapsulated into graphene nanoshells. Then the metal particles fluctuated inside the solid forming small active domains where the GCNT can grow during the pyrolysis process. Consequently, the metal particles were encapsulated in graphene nanoshells either at the tip end or in the cavity. Further extending the holding time, lamellar structure gradually disappeared, and a wide range of longer intertwined tubes appeared over the surface of plates, as the graphitic carbon was used as a nanotube growth source. XRD patterns further confirmed what we surmised. As shown in Figure 2b, the intensity of Ni/NiO gradually strengthened as the holding time increased, suggesting the migration of metal nanoparticles. The growth process of GCNT (at 1000 °C) maintained with different holding time was purposefully explored as well, and the results were in line with the mentioned process (Figure S8). Based on the above discussion, we were delighted to discover that the growth of nanotubes underwent the similar evolution process, that is to say, from graphitic carbon to protrusions (baby nanotubes), finally to typical GCNT.

To confirm the flexibility of this pathway, a series of different biomass based precursors were also employed in this study. The experimental results showed that whatever the carbon source (cellulose, glucose, chitin or sucrose) was, they could form tubes under the same synthesis procedure, indicating the universality of this method (Figure S9). Moreover, the effect of other traditional metals on the morphology control was also investigated. $\text{Fe}(\text{NO}_3)_3 \cdot 9\text{H}_2\text{O}$ and $\text{Co}(\text{NO}_3)_2 \cdot 6\text{H}_2\text{O}$ were behaved as catalyst precursors and the results were displayed in Figure S10. Just as we expected, both Fe and Co could catalyze the formation of tubes under the identical conditions.

In order to evaluate the catalytic performance of the products, we choose the direct dehydrogenation of ethylbenzene to styrene as a model reaction, which is of great commercial significance in the chemical industry.^{5a,5b} The catalytic performances of NiO_x @GCNT, GCNT and GCN were evaluated at 550 °C under atmospheric pressure by using diluted ethylbenzene as reactant (Figure 4 and Figure S11). To fairly assess the catalytic performance of the products, the specific reaction rates as the amount of styrene produced per square meter of surface per hour are calculated. The NiO_x @GCNT exhibit superior activity and give a value of 8.1

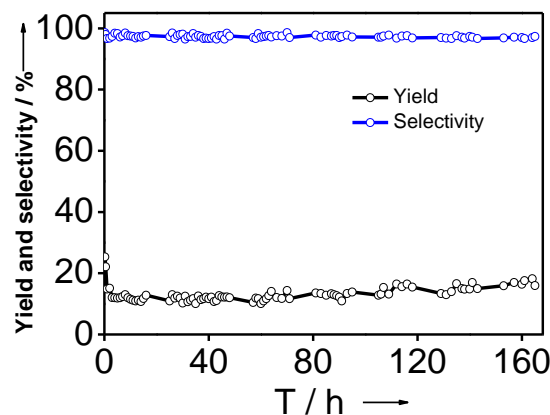


Figure 4. Direct ethylbenzene dehydrogenation activity of NiO_x @GCNT (mass ratio GAH:melamine:Ni=1:20:1.1, 1000 °C).

$\mu\text{molm}^{-2}\text{h}^{-1}$, higher than GCNT ($4.6 \mu\text{molm}^{-2}\text{h}^{-1}$). The yield and selectivity of $\text{NiO}_x@\text{GCNT}$ can reach up to 15.0% and 97.5%, respectively. Amazingly, $\text{NiO}_x@\text{GCNT}$ shows unprecedented stability over 165 h without any activation process, which has never been reported before. A series of characterizations and analysis showed that the surface area, the pore size distribution, the content of C=O and the valence of Ni in $\text{NiO}_x@\text{GCNT}$ and GCNT are comparable (Figure S3, S12). The most difference is that the content of Ni decreased dramatically to 5.5 wt% from 18.4 wt% by acid treatment. We deduced that the improved activity may derived from the synergistic effect of metal and GCNT. The special curvature of GCNT results in a partial Ni carbon covalent bond with a charge transfer from carbon to Ni.²¹ The charge transfer may contribute towards activating the Ni thus leading to a higher activity rate.²¹ Meanwhile, CO_2 -TPD (Figure S13) demonstrated that $\text{NiO}_x@\text{GCNT}$ catalyst is abundant in strong basic sites compared to GCNT, which is another factor for the improved performance.²² Particularly worth mentioning was that the sheet-like GCN exhibited negligible catalytic activity, which suggested that the microstructure of carbon materials made a great difference in catalytic capacity.²² This highly active hybrids catalyst with low cost, handle-convenient and earth abundance is promising for future industrial applications.

To sum up, we have demonstrated a versatile strategy to synthesize CNTs by pyrolysis of biomass/melamine/nitrate mixtures. By exploring the effect of diverse parameters, we concluded that GCNT evolution should proceed via graphitic carbon to protrusions (baby nanotubes), finally to typical GCNT. The early formation of graphitic carbon is conducive to the growth of GCNT, and the fluctuation of active metals catalyzed the growth of GCNT from graphitic carbon. Consequently, the achieved GCNT was endowed with specific graphene-like sidewalls, large inner diameter, and high crystalline and graphitization degree. Additionally, the as-grown $\text{NiO}_x@\text{GCNT}$ exhibit outstanding catalytic performance in the direct dehydrogenation of ethylbenzene (the specific reaction rate can reach up to $8.1 \mu\text{molm}^{-2}\text{h}^{-1}$). In particular, unprecedented stability was shown over 165 h without any activation process. This simple, efficient and cost-competitive synthetic methodology not only highlights the vast opportunities in the fabrication of CNTs with unique morphology, but also stimulates further investigations in the area of catalysis.

Financial support from the National Natural Science Foundation of China (21376208), the Zhejiang Provincial Natural Science Foundation for Distinguished Young Scholars of China (LR13B030001), the Specialized Research Fund for the Doctoral Program of Higher Education (J20130060), the Fundamental Research Funds for the Central Universities, the Program for Zhejiang Leading Team of S&T Innovation, the Fundamental Research Funds for the Central Universities and the Partner Group Program of the Zhejiang University and the Max-Planck Society are greatly appreciated.

Notes and References

- (a) D. Jariwala, V. K. Sangwan, L. J. Lauhon, T. J. Marks, M. C. Hersam, *Chem. Soc. Rev.* 2013, **42**, 2824; (b) X. H. Li, M. Antonietti, *Chem. Soc. Rev.* 2013, **42**, 6593.
- (a) M. F. L. De Volder, S. H. Tawfick, R. H. Baughman, A. J. Hart, *Science* 2013, **339**, 535; (b) H. J. Dai, *Surf. Sci.* 2002, **500**, 218; (c) A. A. Green, M. C. Hersam, *Nat. Nanotechnol.* 2009, **4**, 64.
- (a) S. Y. Wang, E. Iyyamperumal, A. Roy, Y. H. Xue, D. S. Yu, L. M. Dai, *Angew. Chem. Int. Ed.* 2011, **50**, 11756; (b) L. J. Yang, S. J. Jiang, Y. Zhao, L. Zhu, S. Chen, X. Z. Wang, Q. Wu, J. Ma, Y. W. Ma, Z. Hu, *Angew. Chem. Int. Ed.* 2011, **50**, 7132.
- H. Yi, D. Ghosh, M.-H. Ham, J. Qi, P. W. Barone, M. S. Strano, A. M. Belcher, *Nano Lett.* 2012, **12**, 1176.
- (a) J. Zhang, D. S. Su, R. Blume, R. Schloegl, R. Wang, X. Yang, A. Gajovic, *Angew. Chem. Int. Ed.* 2010, **49**, 8640; (b) H. Liu, J. Diao, Q. Wang, S. Gu, T. Chen, C. Miao, W. Yang, D. Su, *Chem. Commun.*, 2014, **50**, 7810; (c) W. Qi, W. Liu, B. S. Zhang, X. M. Gu, X. L. Guo, D. S. Su, *Angew. Chem. Int. Ed.* 2013, **52**, 14224.
- M. S. Jeong, J. H. Han, Y. C. Choi, *Carbon* 2013, **57**, 338.
- M. H. Rummeli, E. Borowiak-Palen, T. Gemming, T. Pichler, M. Knupfer, M. Kalbac, L. Dunsch, O. Jost, S. R. P. Silva, W. Pompe, B. Buchner, *Nano Lett.* 2005, **5**, 1209.
- (a) L. Mieczko, G. Lolli, *Angew. Chem. Int. Ed.* 2013, **52**, 9372; (b) Y. L. Li, I. A. Kinloch, A. H. Windle, *Science* 2004, **304**, 276; (c) S. S. Fan, M. G. Chapline, N. R. Franklin, T. W. Tomblor, A. M. Cassell, H. J. Dai, *Science* 1999, **283**, 512; (d) F. Yang, X. Wang, D. Zhang, J. Yang, D. Luo, Z. Xu, J. Wei, J.-Q. Wang, Z. Xu, F. Peng, X. Li, R. Li, Y. Li, M. Li, X. Bai, F. Ding, Y. Li, *Nature* 2014, **510**, 522; (e) G. Ning, C. Xu, X. Zhu, R. Zhang, W. Qian, F. Wei, Z. Fan, J. Gao, *Carbon*, 2013, **56**, 38.
- A. Kibria, Y. H. Mo, K. S. Nahm, M. J. Kim, *Carbon* 2002, **40**, 1241.
- Z. H. Wen, Q. Wang, J. H. Li, *Adv. Funct. Mater.* 2008, **18**, 959.
- H. Omachi, T. Nakayama, E. Takahashi, Y. Segawa, K. Itami, *Nat. Chem.* 2013, **5**, 572.
- (a) E. O. Pentsak, E. G. Gordeev, V. P. Ananikov, *ACS Catal.* 2014, **4**, 3806; (b) A. Kudo, S. A. Steiner, B. C. Bayer, P. R. Kidambi, S. Hofmann, M. S. Strano, B. L. Wardle, *J. Am. Chem. Soc.* 2014, **136**, 17808.
- (a) J. Zhang, R. Wang, E. Z. Liu, X. F. Gao, Z. H. Sun, F. S. Xiao, F. Girgsdies, D. S. Su, *Angew. Chem. Int. Ed.* 2012, **51**, 7581; (b) D. C. Lee, F. V. Mikulec, B. A. Korgel, *J. Am. Chem. Soc.* 2004, **126**, 4951; (c) M. H. Ruemmel, F. Schaeffel, A. Bachmatiuk, D. Adebimpe, G. Trotter, F. Boerrnert, A. Scott, E. Coric, M. Sparing, B. Rellinghaus, P. G. McCormick, G. Cuniberti, M. Knupfer, L. Schultz, B. Buechner, *ACS Nano* 2010, **4**, 1146; (d) N. T. Alvarez, C. L. Pint, R. H. Hauge, J. M. Tour, *J. Am. Chem. Soc.* 2009, **131**, 15041; (e) Y. Li, R. L. Cui, L. Ding, Y. Liu, W. W. Zhou, Y. Zhang, Z. Jin, F. Peng, J. Liu, *Adv. Mater.* 2010, **22**, 1508.
- Y. Wang, X. C. Wang, M. Antonietti, *Angew. Chem. Int. Ed.* 2012, **51**, 68.
- J. Wang, Z. Xu, Y. Gong, C. Han, H. Li, Y. Wang, *ChemCatChem* 2014, **6**, 1204.
- S. Maldonado, S. Morin, K. J. Stevenson, *Carbon* 2006, **44**, 1429.
- H. Liu, Y. Zhang, R. Y. Li, X. L. Sun, S. Desilets, H. Abou-Rachid, M. Jaidann, L. S. Lussier, *Carbon* 2010, **48**, 1498.
- T. Odedairo, J. Ma, Y. Gu, J. L. Chen, X. S. Zhao, Z. H. Zhu, *J. Mater. Chem. A* 2014, **2**, 1418.
- X.-H. Li, S. Kurasch, U. Kaiser, M. Antonietti, *Angew. Chem. Int. Ed.* 2012, **51**, 9689.
- F. Goettmann, A. Fischer, M. Antonietti, A. Thomas, *Angew. Chem. Int. Ed.* 2006, **45**, 4467.
- (a) X.-F. Guo, J.-H. Kim, G.-J. Kim, *Catal. Today*, 2011, **164**, 336; (b) L. M. Ombaka, P. Ndungu, V. O. Nyamori, *Catal. Today*, 2013, **217**, 65.
- Z. Zhao, Y. Dai, G. Ge, G. Wang, *ChemCatChem*, 2015, **7**, 1135.